Physics in Medicine & Biology

IPEM Institute of Physics and Engineering in Medicine

NOTE

Optimizing the response, precision, and cost of a DNA double-strand break dosimeter

M Obeidat, K McConnell, B Bui, S Stathakis, K Rasmussen, N Papanikolaou, E Y Shim[1] and N Kirby[1,2]

Department of Radiation Oncology, The University of Texas Health Science Center at San Antonio, San Antonio, TX 78229, United States of America

[1] Co-principal investigator.
[2] Author to whom correspondence may be addressed.

E-mail: kirbyn@uthscsa.edu

Abstract

We developed a dosimeter that measures biological damage following delivery of therapeutic beams in the form of double-strand breaks (DSBs) to DNA. The dosimeter contains DNA strands that are labeled on one end with biotin and on the other with fluorescein and attached to magnetic microbeads. Following irradiation, a magnet is used to separate broken from unbroken DNA strands. Then, fluorescence is utilized to measure the relative amount of broken DNA and determine the probability for DSB. The long-term goal for this research is to evaluate whether this type of biologically based dosimeter holds any advantages over the conventional techniques. The purpose of this work was to optimize the dosimeter fabrication and usage to enable higher precision for the long-term research goal. More specifically, the goal was to optimize the DNA dosimeter using three metrics: the response, precision, and cost per dosimeter. Six aspects of the dosimeter fabrication and usage were varied and evaluated for their effect on the metrics: (1) the type of magnetic microbeads, (2) the microbead to DNA mass ratio at attachment, (3) the type of suspension buffer used during irradiation, (4) the concentration of the DNA dosimeter during irradiation, (5) the time waited between fabrication and irradiation of the dosimeter, and (6) the time waited between irradiation and read out of the response. In brief, the best results were achieved with the dosimeter when attaching 4.2 μg of DNA with 1 mg of MyOne T1 microbeads and by suspending the microbead-connected DNA strands with 200 μl of phosphate-buffered saline for irradiation. Also, better results were achieved when waiting a day after fabrication before irradiating the dosimeter and also waiting an hour after irradiation to measure the response. This manuscript is meant to serve as guide for others who would like to replicate this DNA dose measurement technique.

1. Introduction

The improvement of radiation detectors helps to create more accurate, precise, and safer deliveries of ionizing radiation (Seco *et al* 2014). Conventional forms of radiation measurements are made with dosimeters that use chemical and physical approaches to determine the energy deposition by ionizing radiation, and afterwards, correction factors can be required to calculate actual deposition of radiation energy for a patient such as the quality conversion factor and absorbed-dose to water calibration factor (Almond *et al* 1999), yet none of these detectors directly measure biological damage. A DNA dosimeter could provide a more biologically relevant measure of radiation damage following therapeutic delivery by attempting to link radiation dose with a meaningful biological metric.

Radiation induced DNA damage falls into three basic categories: base damage (Klungland *et al* 1999, Fromme and Verdine 2004, Sheila *et al* 2007, Krokan and Bjoras 2013), single-strand break (SSB) (Hutchinson 1985, Peggy 1998, Whitehouse *et al* 2001, Caldecott 2008), and double-strand break (DSB) (Von Sonntag *et al* 1981, Szostak *et al* 1983, Ward 1989, Chu 1997, Jackson 2002, Helleday *et al* 2007). DSBs are difficult to repair and highly toxic compared to base damage and SSBs. DSBs are generally accepted to be one of the dominant factors for

radiation-induced cell killing and could be used as a form of measurement (Chen *et al* 1995). The functionality of the DNA dosimeter is provided through the attachment of a fluorescent marker, fluorescein amidite (6-FAM), to a 4 kilo base-pair (kbp) DNA strand, which is attached to magnetic microbeads (figure 1(a)). After irradiation of the dosimeter (figure 1(b)), a DSB would cause fluorescent ends to fragment and then disperse into the supernatant (see figure 1(c)). Then, broken fluorescent DNA fragments can be separated from the remaining microbeads with unbroken DNA using a magnet, and analysis of fluorescence readings is used to the calculate the probability of DSBs (PDSB). PDSB is defined as the ratio of the fluorescence intensity of the supernatant to the fluorescence intensity of the whole dosimeter. This method of detection has been previously shown to successfully measure DNA DSBs as a function of dose (Obeidat *et al* 2018).

It is important for dosimeter measurements to be precise (Attix 1986) as they can affect interpreted machine dose outputs and therefore also dose delivered to patients. Our goal for the level of precision required for the dosimeter was 1%, which is similar to what can be obtained from other radiation dosimeters that come in batches. We initially faced problems consistently reaching this level of precision. For this reason, the basic aim of this work was to revisit selected steps of the DNA dosimeter fabrication and how we measure its response to improve the reproducibility. There were six main areas of focus: (1) the type of microbeads we attach to the DNA strands, (2) the microbeads to PCR mass ratio during the attachment process, (3) the type of suspension buffer for irradiation of the dosimeter, (4) the concentration of the DNA dosimeter, (5) the waiting time between the fabrication and irradiation of the dosimeter, and (6) the waiting time between irradiation and separation of supernatant and microbeads to measure the response. The optimization metrics used in this study were: the coefficient of variation (CoV) to measure the precision of the response, DNA dosimeter response (PDSB), and cost. The goal of each experiment was to minimize the CoV and cost, while maximizing the response of the DNA dosimeter.

The ultimate goal of this work is to make biologically relevant radiation measurements. Future work will benchmark the DNA dosimeter response against cell survival curves. More specifically, the metric for comparison will be relative biological effectiveness. These types of experiments will be critical in determining the relevance of the DNA dosimeter response. However, optimization experiments such as those performed in this manuscript, are crucial to enable more accurate and cost-effective biological measurements.

2. Methods

2.1. Dosimeter fabrication

To create the DNA dosimeter, 4 kbp DNA was synthesized using polymerase chain reaction (PCR) with a combination of oligonucleotides, fluorescein amidite (6 FAM), and biotin. The sequence itself was a random one from the PRS-316 DNA template. The AT:CG content of the synthesized 4 kbp DNA was 0.54:0.46. The PCR reaction relies on thermal cycling to alternate between heating and cooling the samples through a defined series of temperature steps. Table 1 summarizes the recipe used to create 400 μl of PCR product and table 2 shows the thermal cycle steps used to run the PCR reaction which consists of 35 cycles. The net product of this reaction is 4 kbp double-stranded DNA, which is labeled on one end with biotin and on the other with FAM.

The DNA strands were then attached to magnetic microbeads coated in streptavidin using the manufacturer-recommended immobilization procedure (Thermo Fisher Scientific, Waltham, MA). The amount of PCR product that attaches to the magnetic microbeads significantly decreases as the DNA double strand's length exceeds 2 kbp for common binding buffers. Thermo Fisher Scientific has the dynabeads kilobase binder kit binding buffer that was specifically designed to attach longer DNA strands. The following steps were used to attach the PCR product with 1 mg of magnetic microbeads:

1. 200 μl of washing buffer (10 mM Tris-HCl, pH 7.5, 1 mM EDTA, and 2.0 M NaCl) was added gently to 1 mg of magnetic microbeads and placed inside a micro centrifuge tube to be washed by placing the tube against a magnet, then waiting a few minutes before extracting and discarding the supernatant.
2. The washed magnetic microbeads were resuspended in 200 μl of binding buffer.
3. 100 μl of distilled water and a specific mass of PCR product (see section 2.5) were added to the suspended magnetic microbeads inside the microfuge tube.
4. The mixture was incubated at room temperature for 3 h on a roller to keep the microbeads in suspension. During this, the mixture was covered with aluminum foil to block the room light.
5. The microbead-connected DNA strands were washed twice with 500 μl of washing buffer, then once with 500 μl of elution buffer (10 mM Tris HCl, pH 7.5).
6. The microbead-connected DNA strands were resuspended and stored in 200 μl of washing buffer and refrigerated in the dark.
7. To prepare the dosimeter for irradiation experiments, the storage washing buffer was first discarded, then we resuspended the microbead-connected DNA strands with a specific volume of a buffer
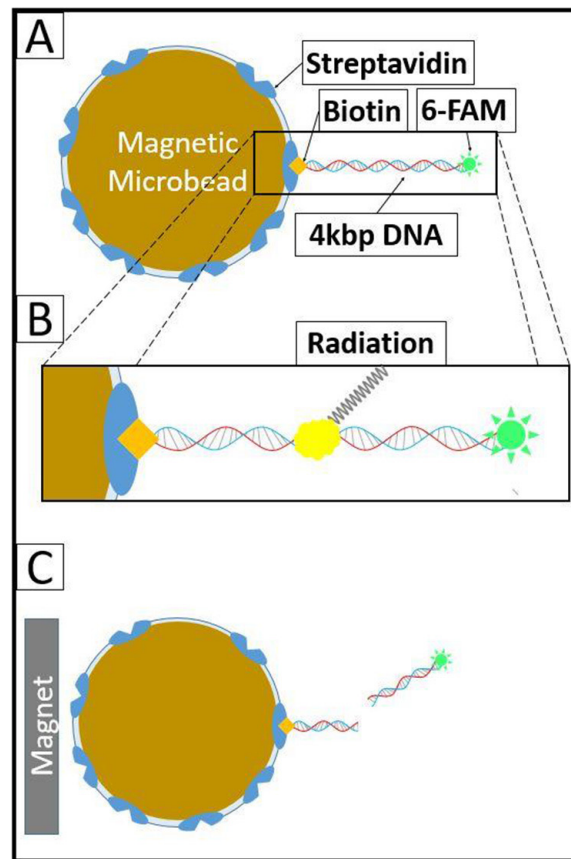
Figure 1. (a) The DNA dosimeter consisting of four basic components: magnetic microbeads, 4 kbp double-stranded DNA, biotin, and 6-FAM. (b) Irradiation of the dosimeter. (c) If a DSB occurs, the fluorescein becomes free and is no longer attached to the microbeads, then a magnet can be used to separate the broken pieces of DNA from the intact ones.

Figure 2. Separating the supernatant and microbeads following irradiation of the DNA dosimeter by placing the irradiated DNA dosimeter against a magnet, then waiting few minutes before extracting the supernatant.

Table 1. The required volume and concentration of materials to create 400 μl of PCR product. U: unit of enzyme activity.

Material	Volume (μl)
Deionized water	334.4
Accu PCR buffer (I)	40
Biotin-pRS316 4kb 5 (10 pmol μl^{-1})	8
FAM-pRS316 3' (10 pmol μl^{-1})	8
PRS 316 (5 ng μl^{-1})	8
Accuprime taq polymerase high fidelity (5 U μl^{-1})	1.6

Table 2. The thermal cycle used to run the PCR reaction. The denaturation, annealing, and elongation steps were repeated 35 times. ∞ denotes a temporary store of the PCR product in the cycler at 12 °C.

	Temperature (°C)	Time on hold (s)
Initialization step	94	15
Denaturation step	94	15
Annealing step	55	15
Elongation step	68	240
Final elongation step	68	300
Final hold step—short term	12	∞

(see section 2.5) and placed in a microtube for irradiation. The irradiated DNA dosimeters had a volume of 50 μl of these suspended microbead-connected DNA double strands.

2.2. Irradiation setups

Irradiation has been performed by 6 MV photons from a Varian linear accelerator. These occurred in one of two phantom setups: a water-equivalent plastic phantom or a water tank. The plastic phantom ($9.3 \times 9.3 \times 10\,\text{cm}^3$) was set up on a tray attached to the linear accelerator head at 57.5 cm source to surface distance (SSD) and the samples were irradiated at 5 cm depth. The water tank ($53 \times 64 \times 53\,\text{cm}^3$) was set up at 60 cm SSD and the samples were irradiated at a 5 cm depth. The majority of the irradiations occurred in the plastic phantom, due to its ease of setup, but some were performed in the water tank when one was already setup that day for other experiments. For both plastic and water setups, the doses were set based on monitor unit hand calculations from our institutional databook and were corrected based on the daily variation of the output of the linac. This daily variation was determined by comparing measurements with a calibrated $0.3\,\text{cm}^3$ Semiflex 31013 ionization chamber (PTW, Freiburg, Germany) in our monthly machine output setup to the baselines acquired at the last annual TG-51 calibration. No correction was performed as this would not affect both the dose deposition and CoV interpreted from the dosimeter readings regardless of the setup we used.

2.3. DSB measurement

Following irradiation of the DNA dosimeter, we used a DynaMag 2 magnet (Thermo Fisher Scientific, Waltham, MA) to separate broken from unbroken DNA. The magnetic field (3500–3700 Gauss) pulls the magnetic microbeads against the side of the tube (figure 2). Then, the supernatant (S), which represents the fluorescein ends that became free from microbeads, was extracted with a pipette and placed in another microtube. The remaining unbroken DNA was resuspended with 50 μl of phosphate buffered saline (PBS) in the original microtube and its fluorescence signal is referred to here as microbeads (B). Then, we placed both supernatant and microbeads in a reader microplate, and we read the fluorescence signal for each using a Synergy 2 fluorescence reader (BioTek, Winooski, VT). PDSB was calculated with the following equation.

$$\text{PDSB} = \frac{S - \text{BG}}{S + B - 2\text{BG}}. \tag{1}$$

The variable S represents the fluorescence of the supernatant (DNA with DSB), B represents the microbeads (DNA without DSB), and BG was the pure PBS fluorescence intensity (related to the background signal).

2.4. Optimization metrics

Three metrics were chosen to be used in the optimization process: precision, dosimeter response, and cost of the DNA dosimeter. CoV is the mathematical metric we utilized to quantify precision of response for the irradiated DNA dosimeters. Each experiment here was repeated at least three total times. For each experiment repeat, the values varied slightly, but the conclusion for parameters leading to the optimal metric remained the same. The data values (average and CoV) presented here are for five dosimeter readings from the final, most-controlled experiment. Calculating metrics from one experiment avoided the inflation of CoV from inter-batch variations. CoV is calculated by dividing the standard deviation of PDSB over the mean value (Faber and Korn 1991, McKay 1932, Reed et al 2002, Chen *et al* 1995, Jackson 2002, Helleday *et al* 2007). A lower value of CoV indicates less variation in response, which means a more precise response of the DNA dosimeter. PDSB was the metric we used to quantify the dosimeter response. A higher value of PDSB not only meant a higher percentage of DSBs, but also a higher signal-to-noise ratio.

The current dose range of the dosimeter only enables precise measurements (CoV ~1%) for doses around 50 Gy and above. For example, at 5 and 10 Gy the CoV is typically around 14% and 7%, respectively (Obeidat *et al* 2018). Performing experiments with this large CoV would make it difficult to assess whether our interventions are improving the system or not. For this reason, we performed the optimization experiments with doses at 50 Gy and above, where we obtain our most precise response.

Variations in the fabrication techniques for many experiments not only affected the precision and response but also the cost of the DNA dosimeter. For this reason, dosimeter cost was considered as a part of the optimization metrics we used in this project. We created a spreadsheet containing the materials, volumes, and cost of each material used in experiments. This spreadsheet was used to calculate the estimated cost per dosimeter for each condition we changed in the optimization experiments.

We performed some preliminary evaluation for the effect of temperature on DSB stability. We saw an increase in response with increasing temperature, but no reduction of CoV. This can be explored in the future work but it is beyond the scope of this work.

2.5. Refinement of the response, precision, and cost of the DNA dosimeter

2.5.1. Type of magnetic microbeads
We attached the PCR product to two different types of microbeads: Dynabeads M-280 and MyOne T1 (Thermo Fisher Scientific, Waltham, MA). Both types differ in both the diameter (2.8 and 1 μm for M-280 and T1, respectively) and the binding efficiency to PCR product. The purpose here was to investigate which type of microbeads enhances the response, CoV, and cost of the DNA dosimeter. A Varian Clinac 23EX was used to deliver dose levels of 50, 100, and 150 Gy to the DNA dosimeters using the water-equivalent plastic phantom irradiation setup.

2.5.2. Microbead to PCR mass attachment ratio
In Step 3 of the dosimeter fabrication, a specific mass of the PCR product was added to 1 mg of microbeads then incubated for few hours to let the DNA double-strands attach to the microbeads. The purpose here was to attach different masses of PCR product (1.1, 2.1, 4.2, 8.4, and 16.8 μg) to 1 mg of microbeads to investigate the appropriate amount of PCR needed to optimize the response, CoV, and cost of the DNA dosimeter. The masses of PCR were calculated by multiplying the concentration of the PCR product by the volume we used in each experiment, and the concentration of PCR was estimated by running gel electrophoresis for different dilutions of the PCR product to find the concentration. A Varian Clinac 23EX was used to deliver 50 Gy to the DNA dosimeters using the water-equivalent plastic phantom irradiation setup.

2.5.3. Type of suspension buffer for irradiation
In Step 7 of the dosimeter fabrication, we suspended the microbead-connected DNA strands with a buffer for irradiation. The purpose here was to test if changing the irradiation buffer will have an effect on the response, precision, and cost of the DNA dosimeter. We suspended the microbead-connected DNA strands with three types of buffer for irradiation: elution buffer (10 mM Tris HCl, pH 7.5), washing buffer (10 mM Tris HCl, pH 7.5, 1 mM EDTA, and 2.0 M NaCl), and PBS (10 mM Na_2HPO_4, 2.7 mM KCl, 137 mM NaCl, and 1.76 mM KH_2PO_4, pH 7.4). A Varian Clinac 23EX was used to deliver dose levels of 50, 100, and 200 Gy to the DNA dosimeters using the water-equivalent plastic phantom irradiation setup.

2.5.4. Irradiation concentration of the DNA dosimeter
In Step 7 of the dosimeter fabrication, the same volume of microbead-connected DNA strands was suspended with different volumes of the buffer (100, 200, and 400 μl) to create different concentrations of the dosimeter. This experiment was performed after we decided what type of suspension buffer we used for irradiation (type of suspension buffer for irradiation experiment). The purpose here was to create different concentrations of the DNA dosimeter to test which one optimized the response, CoV, and cost of the DNA dosimeter. A Varian Clinac 23EX was used to deliver 50 Gy to the DNA dosimeters using the water tank irradiation setup.

2.6. Optimizing the time interval between fabrication, irradiation, and separating the supernatant and microbeads

2.6.1. Time between fabrication and irradiation of the DNA dosimeter
The purpose here was to test the effect of the waiting time between the fabrication and irradiation of the DNA dosimeter on both the response and precision of the DNA dosimeter. After fabricating a batch of the DNA dosimeter, we tested both waiting for an hour and waiting for a day before irradiating the DNA dosimeter with a Varian Clinac 23EX to 50 and 100 Gy using the water-equivalent plastic phantom irradiation setup. This experiment had no impact on the cost of dosimeter.

2.6.2. Time between irradiation and separation of supernatant and microbeads
The time we needed to wait following irradiation of the dosimeter to separate the supernatant and microbeads was investigated here to test the effect on both response and precision of the DNA dosimeter. One batch of the DNA dosimeter was fabricated and a Varian Novalis Tx was used to deliver 50, 100, and 150 Gy to two sets of the same batch using the water tank irradiation setup. For the first set, we separated the supernatant and microbeads

Table 3. The DNA dosimeter response (PDSB) and CoV when attached to different types of microbeads.

	Dynabeads M-280		MyOne T1 beads	
Dose [Gy]	PDSB	CoV	PDSB	CoV
50	0.010	0.43	0.050	0.045
100	0.016	0.07	0.097	0.010
150	0.030	0.04	0.156	0.026

Table 4. The DNA dosimeter response (PDSB), CoV, and cost per dosimeter for different attached masses of PCR to the same amount of microbeads.

PCR mass (μg)	PDSB	CoV	Cost ($)
1.1	0.047	0.15	5.85
2.1	0.059	0.039	6.07
4.2	0.054	0.028	6.50
8.4	0.071	0.12	7.39
16.8	0.058	0.042	9.16

Table 5. The DNA dosimeter response (PDSB) and CoV when suspended with different types of buffer for irradiation.

	Elution buffer		Washing buffer		PBS	
Dose [Gy]	PDSB	CoV	PDSB	CoV	PDSB	CoV
50	0.017	0.23	0.012	0.27	0.048	0.14
100	0.021	0.08	0.039	0.030	0.052	0.023
200	0.025	0.051	0.058	0.028	0.119	0.017

directly following irradiation, while for the second one, we waited an hour before the separation. This experiment had no impact on the cost of dosimeter.

3. Results

3.1. Type of magnetic microbeads
Table 3 shows the DNA dosimeter response and CoV for different dose levels when attached to two different types of microbeads (the cost for both types of microbead is equal). Both the response and CoV of the DNA dosimeter improved when the MyOne T1 microbeads are utilized.

3.2. Microbead to PCR mass attachment ratio
Table 4 shows the DNA dosimeter response, CoV, and cost when attached to different PCR masses during fabrication then irradiated to 50 Gy. The lowest CoV (highest precision of response) was achieved by attaching 4.2 μg of PCR with 1 mg of microbeads.

3.3. Type of suspension buffer for irradiation
Table 5 shows the DNA dosimeter response for different dose levels when suspended with different types of buffer for irradiation. The table shows an enhancement in both the dosimeter response and CoV when suspended with PBS. The cost of the DNA dosimeter for all suspensions was very similar. Figure 3 shows a graphical representation for table 5.

3.4. Irradiation concentration of the DNA dosimeter
Table 6 shows the DNA dosimeter response, CoV, and cost per dosimeter for different concentrations of dosimeters when irradiated to 50 Gy. The CoV was similar for resuspensions with 100 and 200 μl of PBS (0.011 and 0.012, respectively) but the response was higher for the 100 μl suspension (the most concentrated DNA dosimeter).

3.5. Time between fabrication and irradiation of the DNA dosimeter
Table 7 shows the effect of the waiting time between the DNA dosimeter fabrication and irradiation on both the response and CoV for different dose levels. The results indicate that waiting for one day significantly enhanced the CoV changing from 0.16 and 0.13 to 0.045 and 0.010 for 50 and 100 Gy, respectively.
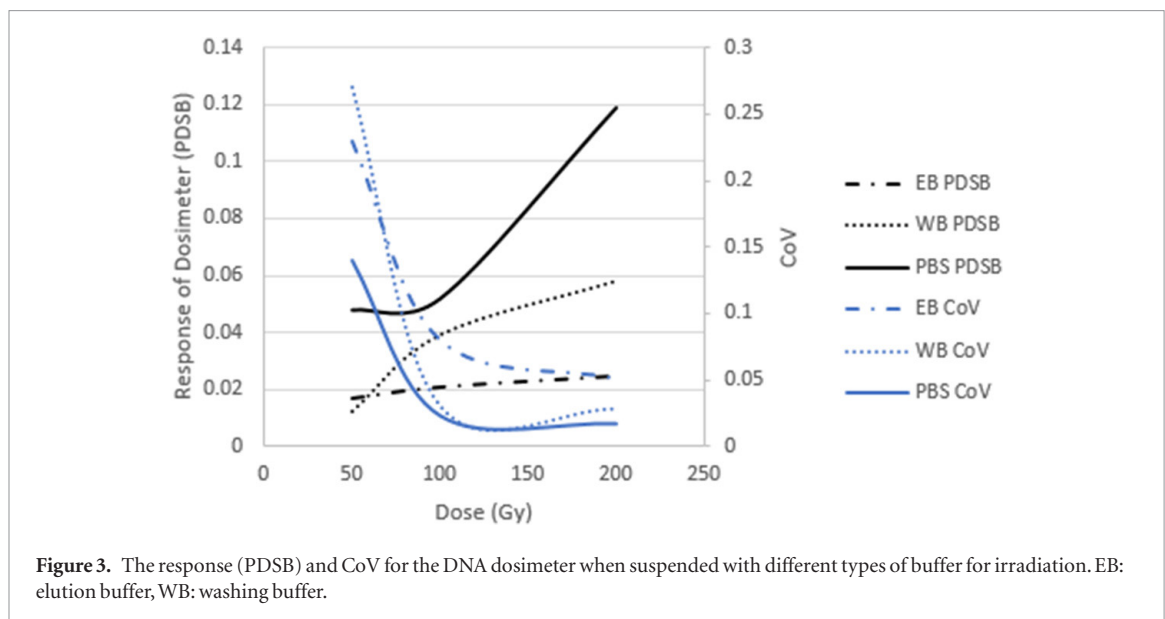
Figure 3. The response (PDSB) and CoV for the DNA dosimeter when suspended with different types of buffer for irradiation. EB: elution buffer, WB: washing buffer.

Table 6. The DNA dosimeter response (PDSB), CoV, and cost per dosimeter for different concentrations of the DNA dosimeter created by suspending the same amount of microbead-connected DNA strands with different volumes of PBS.

100 μl of PBS cost: $13		200 μl of PBS cost: $6.50		400 μl of PBS cost: $3.25	
PDSB	CoV	PDSB	CoV	PDSB	CoV
0.191	0.011	0.116	0.012	0.088	0.043

Table 7. The DNA dosimeter response (PDSB) and CoV when irradiated after an hour and a day after fabrication.

	1 h		1 d	
Dose [Gy]	PDSB	CoV	PDSB	CoV
50	0.060	0.16	0.058	0.045
100	0.089	0.13	0.093	0.010

3.6. Time between irradiation and separation of supernatant and microbeads

Table 8 shows the effect of the waiting time between the DNA dosimeter irradiation and separating the supernatant and microbeads on both the response and CoV for different dose levels. The results indicate that both the response and CoV improved by waiting an hour before we performed the separation.

4. Discussion

The key driving factor of optimizing the DNA dosimeter was to enhance the response and decrease the CoV. Some of the experiments naturally affected the cost. For the microbead to PCR mass attachment ratio experiment, attaching 4.2 μg of PCR product with 1 mg of microbeads produced the lowest CoV and a less expensive DNA dosimeter than if we used higher masses of PCR. For the same experiment, we were able to fabricate a less expensive dosimeter but the compromise here was a lower response and a higher CoV.

For concentration of the DNA dosimeter experiment, the CoV was similar for both 100 and 200 μl PBS suspensions so the key to choosing between these became the cost, the 200 μl PBS suspension produced twice the number of DNA dosimeters with the same total cost and CoV as the 100 μl PBS suspension. Thus, a 200 μl PBS suspension was utilized for the DNA dosimeter. We optimized the cost of the DNA dosimeter by finding the cheapest formula which created a 0.01 CoV for doses around 50 Gy. The cost of the DNA dosimeter is currently at $6.50 per 50 μl dosimeter.

Using PBS enhanced the response of the DNA dosimeter for all dose levels compared to the other buffers we tested. Also, using PBS to suspend the DNA dosimeter samples not only improved the response, but also had a biological advantage as its ions concentration and osmolarity matches the internal environment of our body (isotonic for mammalian cells) (Blomberg *et al* 1980). This match between the PBS and human bodies can be considered as an advantage for the DNA dosimeter.

Table 8. The DNA dosimeter response (PDSB) and CoV when the response is measured without waiting and waiting for one hour later to separate the supernatant and microbeads following irradiation.

Dose [Gy]	No waiting		1 h	
	PDSB	CoV	PDSB	CoV
50	0.051	0.067	0.132	0.017
100	0.092	0.080	0.223	0.013
150	0.178	0.048	0.318	0.021

The effect of the waiting time between fabrication, irradiation, and separation was investigated because of the high CoV we got for some experiments while using the same dosimeter fabrication formula. Finding the appropriate waiting time which produced a lower CoV also helped us to keep a consistency between experiments and excluded a factor that could change the precision of the DNA dosimeter response. We tried many other time periods before this set but the experiments were not systematically controlled well. We noted general trends demonstrating the importance of waiting around a day after dosimeter fabrication before usage and also waiting at least an hour after irradiation before separation. This is why we chose to focus on these time periods for the controlled experiments here.

5. Conclusion

The DNA dosimeter optimization process consisted of testing a number of variables through different experiments. For each variable experiment, we investigated the best condition to produce a higher response, a lower CoV, and a cheaper cost. The best results were achieved with the dosimeter when attaching 4.2 μg of DNA with 1 mg of MyOne T1 microbeads and by suspending the microbead-connected DNA strands with 200 μl of phosphate-buffered saline for irradiation. Beyond this, it was preferable to wait a day after fabrication to irradiate the DNA dosimeter and to wait an hour after irradiation before we separate the supernatant and microbeads to read the response. This generally allowed us to produce a CoV on the order of 0.01 reproducibly with a fabrication cost of \$6.50 for doses around 50 Gy.

Acknowledgments

References

Almond P R *et al* 1999 AAPM's TG-51 protocol for clinical reference dosimetry of high-energy photon and electron beams *Med. Phys.* **26** 1847–70

Attix F H 1986 *Introduction to Radiological Physics and Radiation Dosimetry* (New York: Wiley) pp 277–91

Blomberg B, Bernard C and Du Pasuier L 1980 *In vitro* evidence for T-B lymphocyte collaboration in the clawed toad, *Xenopus Eur. J. Immunol.* **10** 869–76

Caldecott K W 2008 Single-strand break repair and genetic disease *Nat. Rev. Genet.* **9** 619–31

Chen W, Blazek E and Rosenberg I 1995 The relaxation of supercoiled DNA molecules as a biophysical dosimeter for ionizing radiations: a feasibility study *Med. Phys.* **22** 1369–75

Chu G 1997 Double strand break repair *J. Biol. Chem.* **272** 24097–100

Faber D S and Korn H 1991 Applicability of the coefficient of variation method for analyzing synaptic plasticity *Biophys. J.* **60** 1288–94

Fromme J C and Verdine G L 2004 Base excision repair *Adv. Protein Chem.* **69** 1–41

Helleday T, Lo J, van Gent D C and Engelward B P 2007 DNA double-strand break repair: from mechanistic understanding to cancer treatment *DNA Repair* **6** 923–35

Hutchinson F 1985 Chemical changes induced in DNA by ionizing radiation *Prog. Nucleic Acid Res. Mol. Biol.* **32** 115–54

Jackson S P 2002 Sensing and repairing DNA double-strand breaks *Carcinogenesis* **23** 687–96

Klungland A, Matthias H, Gunz D, Constantinou A, Clarkson S G, Doetsch P W, Bolton P H, Wood R D and Lindahl T 1999 Base excision repair of oxidative DNA damage activated by XPG protein *Mol. Cell* **3** 33–42

Krokan H E and Bjoras M 2013 Base excision repair *Cold Spring Harbor Perspect. Biol.* **5** a012583

McKay A T 1932 Distribution of the coefficient of variation and the extended 't' distribution *J. R. Stat. Soc.* **95** 695–8

Obeidat M, McConnell K, Li X, Bui B, Stathakis S, Papanikolaou N, Rasmussen K, Ha C S, Lee S E and Kirby N 2018 DNA double-strand breaks as a method of radiation measurements for therapeutic beams *Med. Phys.* **45** 3460–5

Peggy O L 1998 The role of DNA single- and double-strand breaks in cell killing by ionizing radiation *Radiat. Res.* **150** S42–51

Reed G F, Lynn F and Meade B D 2002 Use of coefficient of variation in assessing variability of quantitative assays *Clin. Vaccine Immunol.* **9** 1235–9

Seco J, Clasie B and Partridge M 2014 Review on the characteristics of radiation detectors for dosimetry and imaging *Phys. Med. Biol.* **59** R303

Sheila S D, Valerie L O and Sucharita K 2007 Base-excision repair of oxidative DNA damage *Nature* **447** 941–50

Szostak J W, Orr-Weaver T L, Rothstein R J and Stahl F W 1983 The double-strand-break repair model for recombination *Cell* **33** 25–35

Von Sonntag C, Hagen U, Schon-Bopp A and Schulte-Frohlinde D 1981 Radiation-induced strand breaks in DNA: chemical and enzymatic analysis of end groups and mechanistic aspects *Adv. Radiat. Biol.* **9** 109–42

Ward J F 1989 The yield of DNA double-strand breaks produced intracellularly by ionizing radiation: a review *Int. J. Radiat. Biol.* **57** 1141–50

Whitehouse C J *et al* 2001 XRCC1 stimulates human polynucleotide kinase activity at damaged DNA termini and accelerates DNA single-strand break repair *Cell* **104** 107–17